Thermochronological constraints on two pulses of Cenozoic high-K magmatism in eastern Tibet

WANG Jianghai (王江海)[1], YIN An (尹 安)[2], T. M. Harrison[2], M. Grove[2], ZHOU Jiangyu (周江羽)[1], ZHANG Yuquan (张玉泉)[1] & XIE Guanghong (解广轰)[1]

1. Guangzhou Institute of Geochemistry, Chinese Academy of Sciences, Guangzhou 510640, China;
2. Department of Earth & Space Sciences and Institute of Geophysics & Planetary Physics, University of California, Los Angeles, CA 90095-1567, USA

Correspondence should be addressed to Wang Jianghai (email: wangjh@gig.ac.cn)

Received July 28, 2002

Abstract The previously published U-Pb and $^{40}Ar/^{39}Ar$ ages and our 21 newly-obtained $^{40}Ar/^{39}Ar$ ages suggest that the Cenozoic magmatism in eastern Tibet and Indochina occurred in two episodes, each with distinctive geochemical signatures, at (40—28) Ma and (16—0) Ma. The older rocks are localized along the major strike-slip faults such as the Jinsha-Red River fault system and erupted synchronously with transpression. The younger rocks are widely distributed in rift basins and coeval with the east-west extension of Tibet and eastern Asia. Combining with their geochemical data, we consider that the earlier magmatic phase was generated by continental subduction, while the later volcanic phase was caused by decompression melting of a recently metasomatically-altered, depleted mantle source. The magmatic gap between the two igneous pulses represents an important geodynamic transition in the evolution of eastern Tibet, from the processes controlled mainly by crustal deformation to those largely dominated by mantle tectonics.

Keywords: high-K magmatism, thermochronology, eastern Tibet.

Cenozoic high-K magmatism was vigorously activated in eastern Tibet and controlled by the Early Tertiary pull-apart basins induced by strike-slip faults or Late Tertiary-Quaternary rift basins. These small plutons, dykes and volcanic rocks spatially appear in an intermittent fan-shaped zone[1—3] (fig. 1). Their rock types mainly include ultrapotassic-shoshonitic trachyte, andersitic trachyte, lamprophyre, basanite and syenite, and high-K calc-alkaine alkali basalt and trachy andesite[2—9]. Most previously published ages of Cenozoic high-K rocks in eastern Tibet were determined by the K-Ar method[1,2,4,5,10,11]. Owing to the defects of the K-Ar method[12], the previously published chronological data cannot still be used to establish the precise temporal coordinate for high-K magmatic activities in eastern Tibet. More recently, a few researchers reported some $^{40}Ar/^{39}Ar$ ages of high-K rocks in eastern Tibet[2,6—8], but the dated rocks are dominantly localized in Vietnam[6,8] and formed at 30—40 Ma[2,7]. In this paper, an attempt is made to establish the temporal coordinate for the two pulses of Cenozoic high-K activities, on the basis of our 21 newly-obtained $^{40}Ar/^{39}Ar$ ages and the compilation of the previously published $^{40}Ar/^{39}Ar$ and U-Pb ages.

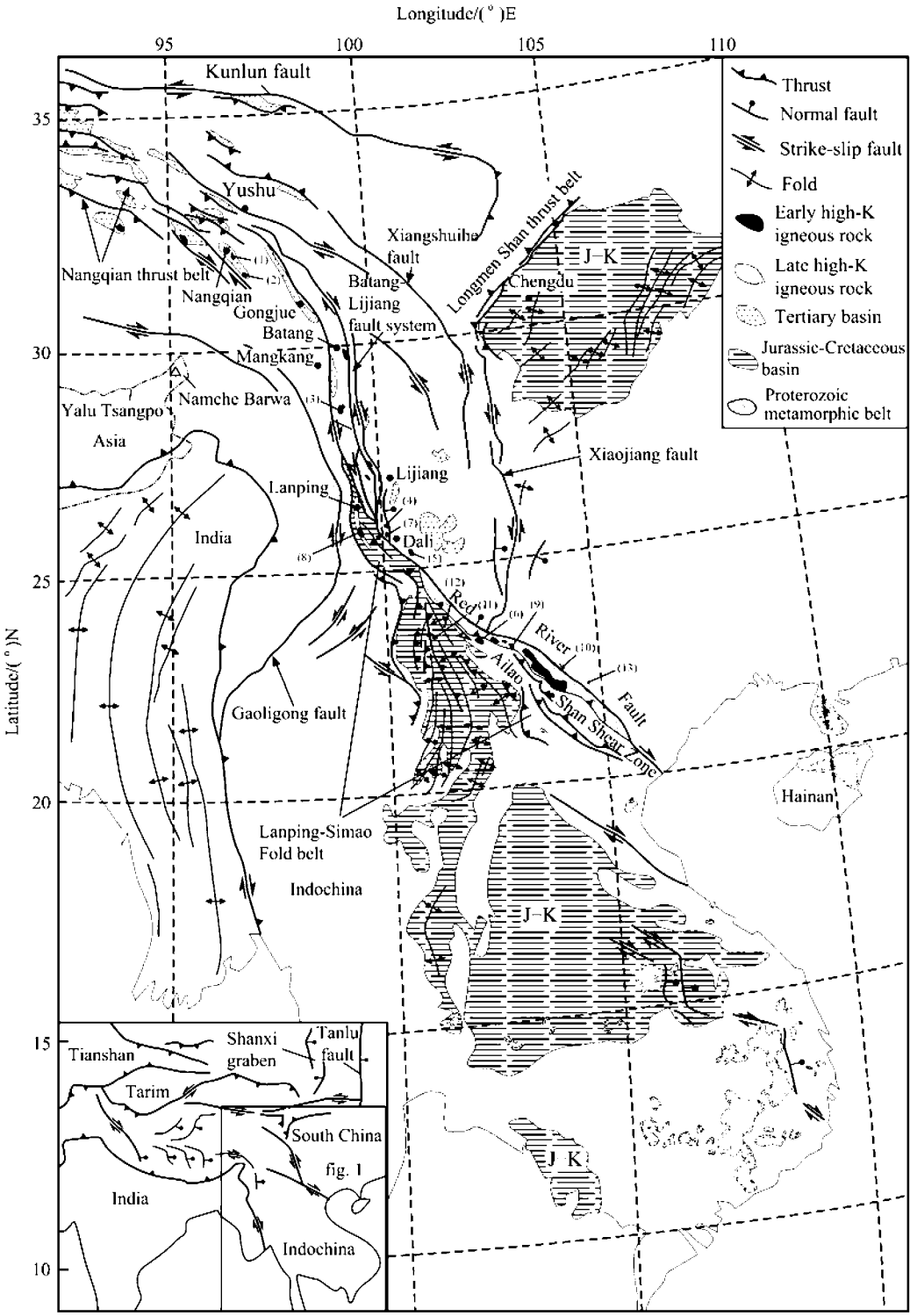

Fig. 1. Cenozoic tectonic map of eastern Tibet and Indochina, illustrating the deformation, distribution of high-K magmatism and localities of sampling. (1)—(13), Sampling localities (see the footnotes of table 1). J-K, Jurassic-Cretaceous strata.

1 Sampling and analytical methods

All of the dated rocks are very fresh and were collected from eastern Tibet. Their detailed localities are indicated in fig. 1 and the footnotes of table 1. We did our best to select K-bearing minerals to time their $^{40}Ar/^{39}Ar$ ages. When K-bearing minerals cannot be separated, some volcanic whole-rocks were also used to date their $^{40}Ar/^{39}Ar$ ages. The K-bearing minerals such as biotite, phlogopite, K-feldspar and K-nepheline were separated from fresh high-K rocks, using a conventional magnetic isodynamic separator and final handpicking under clean environmental conditions after washing and crushing.

A phlogopite separated from sample S8-4 was wrapped in the Al foil and irradiated in Reactor 902 in Mianyang (China), together with a biotite standard (ZBH-2506). Its Ar isotopic compositions were analyzed on an MM-1200 gas mass spectrometer at the Guangzhou Institute of Geochemistry, the Chinese Academy of Sciences (GIG-CAS). The rest separates and whole-rocks were packed in the Sn or Cu foil and sealed in 6-mm-ID evacuated quartz-glass vials, together with the Fish Canyon sanidine (FC-3) flux monitor, and irradiated in the Ford Reactor at the University of Michigan. Their Ar isotopic compositions were measured with a VG 3600 or MM 1200S gas mass spectrometer at the University of California, Los Angeles (UCLA). For detailed analytical procedures, refer to refs. [13, 14]. Because we adopted the monitoring of standards and parallel samples during the course of measurements, the age results obtained in the two different argon labs are comparable.

2 Results and discussion

2.1 Thermochronological result

The $^{40}Ar/^{39}Ar$ dating results of 21 high-K rocks are summarized in table 1. The age spectra for 4 representative samples are presented in fig. 2. Owing to the rapid cooling for high-K volcanic rocks, the $^{40}Ar/^{39}Ar$ ages of whole-rocks or mineral separates should record the time of volcanic eruption. Regarding to the high-K plutons, their $^{40}Ar/^{39}Ar$ ages of whole-rocks or mineral separates only record the time of cooling below closure temperatures. The dated high-K intrusive rocks were collected from the small plutons with the porphyroblastic texture, indicating a relatively rapid cooling. Thus, the cooling ages are close to their emplacement time. In order to overcome the influence of excess argon, most isochron ages are adopted to represent the time of Cenozoic high-K activities. If no good isochron but a plateau is yielded, the plateau age could reflect the time of magmatism, e.g. samples Y-9, XPL-1, MK75-2 and ZP-5. If neither a good isochron nor a plateau appears, its weighted mean age could reflect its time, e.g. samples XT-1 and XP-1. A V-shaped valley in the low-temperature age spectra occurs for sample ZP-5, indicating that it may have resulted from a later thermal disturbance. Thus, its plateau age may represent the time of magmatism.

The age-frequency histogram (fig. 3) for our 21 newly-obtained high-quality $^{40}Ar/^{39}Ar$ ages,

Table 1 Summary of the $^{40}Ar/^{39}Ar$ age data for Cenozoic high-K magmatism in eastern Tibet

Sample No.	Locality in fig. 1[a)]	Rock type[b)]	Dated phase[c)]	Weight /mg	J_0 factor	Total gas age /Ma±σ	Weighted mean /Ma±σ	Plateau age /Ma±σ	Isochron age /Ma±σ	$(^{40}Ar/^{36}Ar)_0$ ±σ	N[d)]
#96-17	(1)	TC	Wr	48.7	0.006971	33.4 ± 0.3	33.1 ± 0.2	32.9 ± 0.2	32.9 ± 0.2	326.2 ± 3.2	14
S7-1	(1)	TC	Wr	23.5	0.007836	38.7 ± 0.6	37.0 ± 0.7	37.9 ± 0.6	36.7 ± 0.9	311.4 ± 8.0	9
S8-4	(1)	LP	Phl	612.9	0.010662	39.0 ± 2.9	39.0 ± 0.3	38.0 ± 0.4	37.2 ± 0.7	323.6 ± 2.0	13
ZM-2	(2)	LP	Phl	6.2	0.007608	37.6 ± 0.3	37.8 ± 0.2	37.7 ± 0.1	37.8 ± 0.2	294.3 ± 2.7	11
MK391-6	(3)	TC	Wr	47.5	0.006929	34.0 ± 0.2	34.0 ± 0.3	33.7 ± 0.2	32.8 ± 0.9	340.2 ± 4.7	10
MK75-2	(3)	TC	Wr	26.2	0.007520	32.3 ± 0.2	33.8 ± 0.7	33.3 ± 0.1	34.8 ± 0.3	139.7 ± 41.3	12
G035-1	(4)	ST	Kf	12.3	0.007904	37.2 ± 0.4	37.1 ± 0.4	37.0 ± 0.1	37.0 ± 0.4	297.7± 6.4	18
G035-2	(4)	ST	Kf	11.5	0.007902	37.4 ± 0.5	37.0 ± 0.4	37.3 ± 0.3	36.8 ± 0.4	302.0 ± 1.6	15
G035-3	(4)	ST	Kf	7.2	0.007903	38.2 ± 0.4	37.4 ± 0.5	37.1 ± 0.2	37.0 ± 0.4	304.4 ± 6.1	15
G035-4	(4)	ST	Kf	6.6	0.006911	34.2 ± 1.1	32.8 ± 0.7	32.2 ± 0.9	30.8 ± 0.8	321.0 ± 3.4	15
G035-5	(4)	ST	Kf	6.0	0.007507	35.8 ± 0.5	35.0 ± 0.3	35.0 ± 0.3	34.6 ± 0.3	299.6 ± 2.1	13
MC1-1	(5)	ST	Kf	6.3	0.006890	31.6 ± 0.6	30.6 ± 0.4	30.6 ± 0.5	29.1 ± 0.5	358.3 ± 6.5	15
LWZ-1	(6)	LP	Phl	5.2	0.006929	32.1 ± 0.4	31.5 ± 0.4	31.7 ± 0.4	30.8 ± 0.4	326.4 ± 4.8	8
Y-9	(7)	ST	Wr	50.0	0.006863	29.5 ± 0.3	30.6 ± 0.5	29.4 ± 0.3	29.8 ± 0.8	361.1 ± 7.0	9
ZP-5	(8)	ST	Ne	29.4	0.007882	36.6 ± 0.4	32.0 ± 1.6	36.9 ± 0.2	24.1 ± 0.2	688.6 ± 2.3	17
DP1-1	(9)	BTA	Kf	7.9	0.006917	34.5 ± 0.4	33.7 ± 0.4	34.4 ± 0.4	33.3 ± 0.4	313.2 ± 2.8	6
DP19-1	(9)	BTA	Bt	8.0	0.006902	35.1 ± 0.5	35.8 ± 0.8	35.2 ± 0.5	34.0 ± 1.2	315.9 ± 3.8	4
XP-1	(10)	BTA	Wr	57.4	0.006967	3.1 ± 0.4	1.3 ± 0.7	–	–	–	9
XPL-1	(11)	BTA	Wr	33.6	0.007424	0.9 ± 0.3	0.8 ± 0.1	0.8 ± 0.2	1.5 ± 0.6	275.2 ± 16.4	8
XT-1	(12)	BTA	Wr	43.7	0.006972	1.8 ± 0.3	1.9 ± 0.3	1.4 ± 0.3	1.0 ± 0.7	343.2 ± 12.9	6
Ma-103	(13)	BN	Phl	8.1	0.006931	12.4 ± 0.2	12.3 ± 0.1	12.3 ± 0.2	11.9 ± 0.3	322.1 ± 14.3	6

a) (1), Nangqian basin; (2), Zhama; (3), Mangkang basin; (4), Laojunshan (Lijiang); (5), Machangqing; (6), Laowangzhai gold deposit; (7), Dali; (8), Zhuopan; (9), Daping; (10), Pingbian; (11), Puer; (12), Tongguan; (13), Maguan. b) TC, trachyte; LP, lamprophyre; ST, syenite; BTA, basaltic trachyandesite; BN, basanite. c) Wr, whole-rock; Phl, phlogopite; Kf, K-feldspar; Ne, nepheline; Bt, biotite. d) N, the number of heating steps.

together with previously published 63 $^{40}Ar/^{39}Ar$ and 3 U-Pb ages[2,6—8,15,16], shows two distinctive magmatic episodes in eastern Tibet: one is between 40 and 28 Ma, and the other since 16 Ma (fig. 3). The high-K magmatism essentially ceased at 28—16 Ma.

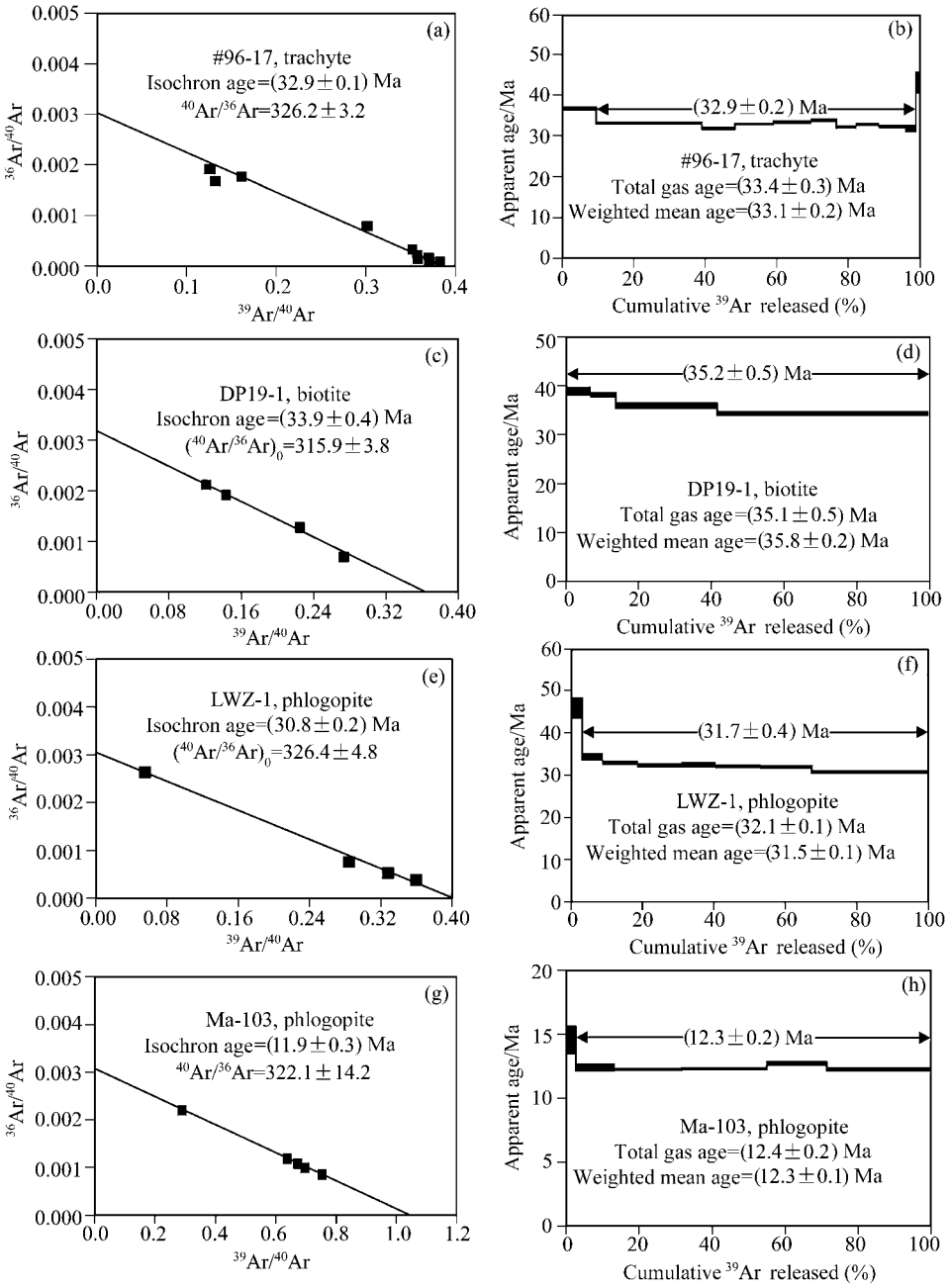

Fig. 2. $^{40}Ar/^{39}Ar$ inverse isochrons and plateau spectra for the four representative high-K magmatic rocks in eastern Tibet.

2.2 Petrogenesis of high-K rocks in eastern Tibet

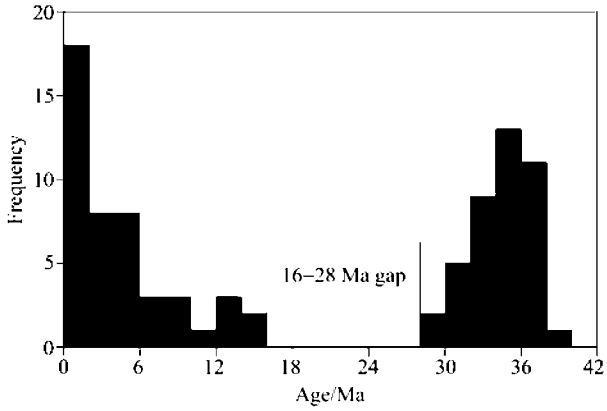

Fig. 3. Age-frequency histogram of Cenozoic high-K rocks of the two phases in eastern Tibet and Indochina.

The older high-K rocks (40—28 Ma) are distributed along the entire Red River shear zone and its northern extension, the Batang-Lijiang fault system and the Nangqian thrust belt (fig. 1). Their rock types include syenite, trachyte, andesitic trachyte and shoshonitic lamprophyre[3,5,10]. Compositionally, the earlier phases of high-K rocks are characterized by relatively low TiO_2 (<1.0%), P_2O_5 (<0.6%) and FeO* (<9%), and high Na_2O (1.3%—5.1%) and K_2O (3.4%—5.2%), enriched with high contents of incompatible trace elements. Most of them are ultra-potassic and shoshonitic, and a few are high-K calc-alkali. Some chondrite-normalized REE patterns of the earlier phase show weakly negative Eu anomalies[17,18], suggesting that plagioclase is a major phase involved in fractional crystallization. This is consistent with the petrographical observation that plagioclase is one of the phenocrysts. The primitive mantle-normalized spidergrams of trace elements exhibit pronounced negative anomalies in Nb, Ta, Ti and P, indicating the involvement of a subduction-related component in the earlier phase[3,18]. The following evidence of tectonic deformation supports the above inference. The previous studies indicated that transpression occurred in eastern Tibet during Eocene-Oligocene (~40—24 Ma)[2]. The Early Mid-Tertiary development of the Lanping-Simao fold belt (fig. 1) and associated development of Late Eocene-Late Oligocene compressional basins indicate that this region was undergoing contraction[3]. The proposed kinematic link between the development of the Lanping-Simao fold belt and the left-slip ductile shearing along the Red River shear zone[19] implies that transpressional tectonics in the Red River region may have started as early as ~40 Ma. Similarly, the northern extension of the Red River shear zone along the Batang-Lijiang fault system also underwent an east-west contraction during Paleogene[20]. The east-west contraction in the north and transpression in the south along north- and northwest-striking strike-slip fault systems along the eastern margin of Tibet gave way to the transtension in the latest Oligocene. They have high $^{87}Sr/^{86}Sr$ (0.705—0.710), $^{206}Pb/^{204}Pb$ (18.52—19.17), $^{207}Pb/^{204}Pb$ (15.78—15.60) and $^{208}Pb/^{204}Pb$ (38.56—39.98) ratios, but low $^{143}Nd/^{144}Nd$ (0.5120—0.5126) ratios[3—5,10]. Their Nd and Sr isotopic compositions lie in the enriched extension of the mantle array, but fall far outside the fields of MORB and Hawaiian basalts. The similarity in Nd and Sr isotopic compositions between the earlier high-K rocks and Tengchong volcanic rocks in western Yunnan indicates that they were derived from the same magmatic source. The Sr-Pb and Nd-Pb isotopic data also plot

outside the field of oceanic basalts. The above signatures of Pb, Sr and Nd isotopes argue against exclusively asthenospheric or mantle plume sources. No correlation between $^{207}Pb/^{204}Pb$ and Ce/Pb or between $^{143}Nd/^{144}Nd$ and Ta/Nd or Ba/Nb ratios also argues against the mixing of asthenospheric and highly enriched lithospheric sources. In $^{87}Sr/^{86}Sr$ vs. $^{206}Pb/^{204}Pb$ and $^{143}Nd/^{144}Nd$ vs. $^{206}Pb/^{204}Pb$ diagrams, the data mainly plot in or near the EM2 field. This indicates that the earlier phase may be derived from an EM2 mantle. However, a few data deviate from the EM2 field, suggesting an input of continental materials with low $^{206}Pb/^{204}Pb$ and $^{143}Nd/^{144}Nd$ ratios and high $^{87}Sr/^{86}Sr$ ratios into mantle-derived melts. The high $^{87}Sr/^{86}Sr$ and low $^{143}Nd/^{144}Nd$ isotope signatures, together with the characteristics of elemental geochemistry, suggest that the earlier phase be derived from a metasomatized subcontinental lithospheric mantle source[17,21].

In contrast, the younger phase (16—0 Ma) is distributed along the southern segment of the active Red River fault and in the Indochina block to the south (fig. 1). Systematic dating of Neogene-Quaternary intraplate activities in the Indochina block[8] reveals essentially continuous basaltic eruptions since ~16 Ma, coinciding with cessation of sea-floor spreading in the South China Sea[22] and termination of transtension along the Red River shear zone at ~17 Ma[14]. The lithotypes of later phase contain alkali basalt, basanite, trachy basalt and trachy andesite.

The geochemistry of the younger phase is characterized by high-K calc-alkali or shoshonitic compositions. They are high in TiO_2 (> 2%), P_2O_5 (> 0.6%), FeO* (> 9%), Na_2O (2.4%—4.0%), K_2O (2%—5%) and incompatible trace elements. The positive anomalies in Nb and Ta, high Ce/Pb (10.44—23.88) and Nb/U (36.07—65.82), and low La/Nb (0.38—0.53) indicate a similarity to oceanic island basalts[17]. They have low $^{87}Sr/^{86}Sr$ (0.703—0.705), $^{206}Pb/^{204}Pb$ (18.17—18.39), $^{207}Pb/^{204}Pb$ (15.51—15.57) and $^{208}Pb/^{204}Pb$ (38.03—38.69), but high $^{143}Nd/^{144}Nd$ (0.5127—0.5131). Nd and Sr isotopic compositions of these rocks plot in or near the MORB quadrant. The striking resemblance in Nd and Sr isotopic compositions between the younger phase and Hawaiian basalts strongly argues against significant crustal contamination. Thus, we consider that the geochemistry of the younger phase nearly reflects its original source compositions without significant continental contamination or fractional crystallization during magma ascent. If the magmatic melts were derived from an enriched Precambrian mantle, these igneous rocks would be characterized not only by high contents of K_2O and incompatible elements, but also by relatively high $^{87}Sr/^{86}Sr$ and low $^{143}Nd/^{144}Nd$ ratios. However, the apparent decoupling between isotopic and elemental compositions indicates that the younger phase was derived from a depleted mantle source enriched by recent mantle metasomatism. The Sr-Pb and Nd-Pb isotopic compositions of the younger phase clearly reflect a hybrid of $^{206}Pb/^{204}Pb$-poor EM1 and MORB mantle sources.

To explain the episodic activities, geochemical characteristics and tempo-spatial relationships to the major structures in eastern Tibet, we propose a new three-stage genetic model (fig. 4)[3]. First, contraction along the Batang-Lijiang fault system and development of the Lanping-Simao fold belt in the Early Tertiary caused local continental subduction along the Red River shear

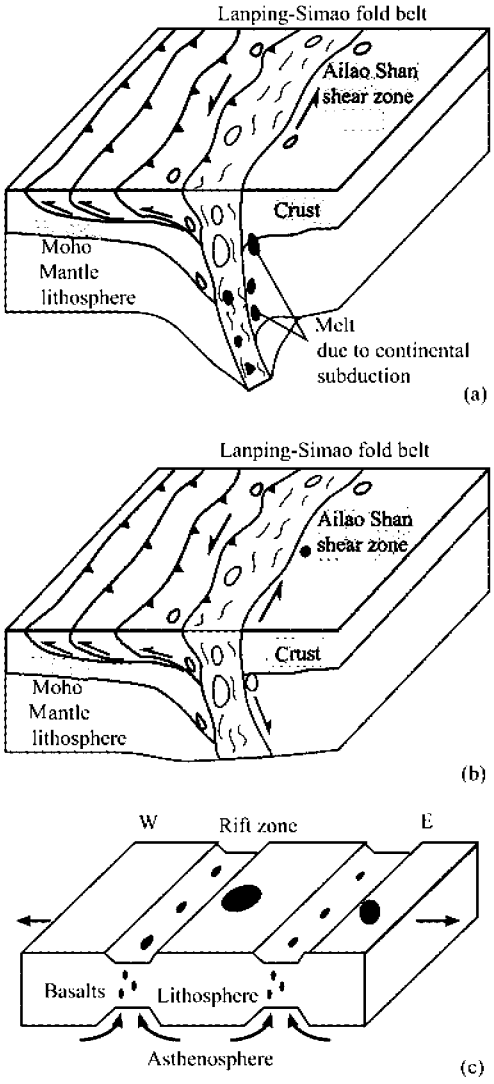

Fig. 4. A new tectonic model for the occurrence of the three tectono-magmatic phases in eastern Tibet and SE Asia. (a) Continental subduction-related magmatism during transpression along the Ailao Shan-Red River shear zone; (b) a magmatic gap during transtension along the Ailao Shan-Red River shear zone; (c) partial melting in the asthenosphere in the Red River region and SE Asia, which caused the younger phase of volcanism.

zone[19], leading to fluid infiltration into the overlying mantle wedge and subsequent melting to generate high-K magma (fig. 4(a)). We interpret the narrow belt of Late Paleocene to Early Miocene basins in eastern Tibet, from the Nangqian thrust belt to the Lanping-Simao fold belt (fig.1), as representing the foreland basins formed by transpression (fig. 1). This proposal is similar to Meyer et al.'s[23] model for northern Tibet. The interpretation of Cenozoic strata in eastern Tibet as contraction-related deposits appears plausible for the Nangqian thrust belt to the north and the Lanping-Simao fold belt to the south where Cenozoic strata are clearly associated with thrusting and folding[2,24] (fig. 1). However, it has recently been suggested[7] that the Paleogene igneous activity in eastern Tibet is due to convective removal of the lower lithosphere beginning at ~40 Ma, this mechanism has been shown to be physically implausible[25].

The U-Pb dating of leucogranites in the Ailao Shan belt indicates that the actual crustal magmatism was sustained till 25 Ma[16]. Thus, there is a magmatic gap of 24—16 Ma. The hiatus coincides with an interval of transtension along the Red River shear zone[14] between 24 Ma and 17 Ma. In addition to halting the flux of volatiles into the underlying mantle wedge, the transition to transtension may have also thinned or removed the crustal root created during the earlier phase of transpression (fig. 4(b)), substantially restricting the conditions appropriate for generating activities.

The younger phase is temporally associated with the widely distributed east-west extension in eastern Tibet and Indochina since the Late Miocene (fig. 4(c))[26]. Along the Red River fault, this is manifested by the development of several north-striking normal faults that merge with the coeval right-slip Red River fault (fig. 1)[24]. This relationship between north-south striking normal faults and west-northwest-striking right-slip faults is similar to that observed in southern Tibet

(fig. 1)[27]. This newly established tectonic regime is not restricted to eastern Tibet, but is widespread throughout eastern Asia. In Tibet, the significant east-west extension began at about 8—4 Ma[28], although local extension may have occurred earlier[29]. Although morphology of rift shoulders in Tibet implies that the active east-west extension is restricted to the upper crust[29], normal-faulting earthquakes at mantle depths[30] and wide spacing of major Tibetan rifts[31] all indicate that the Tibetan extension involves the mantle lithosphere. In North China, the north-south trending Shanxi graben began to develop at about 6 Ma[3]. In SE Siberia, the Baikal rift initiated since 10 Ma and was most active between 8 Ma and 4 Ma[32]. Obviously, most of these eastern Asian rifts are associated with basaltic eruptions and mantle earthquakes, implying that extension is related to asthenospheric flow[29,33,34]. Thus, the new tectonic setting for the occurrence of the 16—0 Ma magmatic activity may represent a fundamental change in geodynamic setting of the Indian and Asian plates.

2.3 Discussion

Cenozoic magmatic activities in eastern Tibet and Indochina occurred in two episodes, each with distinctive geochemical signatures, at 42—24 Ma and 16—0 Ma. The older magmatism is localized along the major strike-slip faults such as the Red River fault system and erupted synchronously with transpression. The younger magmatism is widely distributed in rift basins and coeval with east-west extension in Tibet and entire eastern Asia. The geochemical evidence suggests that the earlier phase was generated by continental subduction, while the younger episode was caused by decompression-induced melting of a metasomatically altered, depleted mantle. The magmatic gap between the two magmatic sequences represents an important geodynamic transition in the evolution of eastern Tibet, from the deformation controlled by crustal processes to that largely dominated by mantle processes.

Acknowledgements This work was jointly supported by the National Natural Science Foundation of China (Grant No. 49972026), the Natural Science Foundation of Guangdong (Grant No. 990531), the projects of the Chinese Academy of Sciences (Grant Nos. KZCX2-SW-117 and KZCX2-101), the Chinese National Key Project for Basic Research (Grant No. G1998040800) and US NSF. We are grateful for insightful reviews by two anonymous referees, who helped to clarify the manuscript.

References

1. Zhang, Y. Q., Xie, Y. W., Tu, G. C., Preliminary studies of the alkali-rich intrusive rocks in the Ailaoshan-Jinshajiang belt and its bearing on rift tectonics, Acta Petrol. Sinica (in Chinese), 1987, (3): 17—25.
2. Pan, G. T., Wang, P. S., Xu, Y. R. et al., Cenozoic tectonic evolution of Qinghai-Xizang Plateau (in Chinese), Beijing: Geological Publishing House, 1990, 32—70.
3. Wang, J. H., Yin, A., Harrison, T. M. et al., A tectonic model for Cenozoic igneous activities in the eastern Indo-Asian collision zone, Earth Planet. Sci. Lett., 2001, 188: 123—133.
4. Deng, W. M., Cenozoic Intraplate Volcanic Rocks in the Northern Qinghai-Xizang Plateau (in Chinese), Beijing: Geological Publishing House, 1998, 1—180.
5. Deng, W. M., Huang, X., Zhong, D. L., Alkali-rich porphyry and its relation with intraplate deformation of the north part of the Jinsha River belt in western Yunnan, China, Science in China, Ser. D, 1998, 41(3): 297—315.
6. Chung, S. L., Lee, T. Y., Lo, C. H. et al., Intraplate extension prior to continental extrusion along the Ailao Shan-Red River

shear zone, Geology, 1997, 25: 311—314.
7. Chung, S. L., Lo, C. H., Lee, T. Y. et al., Diachronous uplift of the Tibetan plateau starting 40 Myr ago, Nature, 1998, 394: 769—773.
8. Lee, T. Y., Lo, C. H., Chung S. L. et al., $^{40}Ar/^{39}Ar$ dating result of Neogene basalts in Vietnam and its tectonic implication, in Mantle Dynamics and Plate Interactions in East Asia (eds. Flower, M. F. J., Chung, S. L., Lo, C. H.), Washington D.C.: AGU, 1998, Geodynamics Ser. 27: 317—330.
9. Wang, J. H., Xie, G. H., Yin, A. et al., Geochemistry and thermochronology of alkali volcano-intrusive complexes in eastern Tibet and Yunnan, in Mineral Resources, Environment and Sustainable Development (ed. Institute of Geochemistry, Chinese Academy of Sciences) (in Chinese), Beijing: Science Press, 1999, 387—388.
10. Zhang, Y. Q., Xie, Y. W., Geochronology of Ailaoshan-Jinshajiang alkali-rich intrusive rocks and their Sr and Nd isotopic characteristics, Sci. in China, Ser. D, 1997, 40(5): 522—529.
11. Deng, W. M., Sun, H. J., Zhang, Y. Q., K-Ar age of Cenozoic volcanic rocks in the Nangqian Basin, Qinghai Province and its geological significance, Chinese Sci. Bull., 2000, 45(11): 1014—1019.
12. McDougall, I., Harrison, T. M., Geochronology and Thermochronology by the $^{40}Ar/^{39}Ar$ Method, New York: Oxford University Press, 1999, 1—269.
13. Dai, T. M., Hong, A. S., $^{40}Ar/^{39}Ar$ dating and some isotopic determinations on Himalaya biotites from granitoids rocks in southern Tibet, Geochimica (in Chinese), 1982, 11: 48—55.
14. Harrison, T. M., Leloup, P. H., Ryerson, F. J. et al., Diachronous initiation of transtension along the Ailao Shan-Red River shear zone, Yunnan and Vietnam, in The Tectonic Evolution of Asia (eds. Yin, A., Harrison, T. M.), New York: Cambridge University Press, 1996, 208—226.
15. Schärer, U., Zhang, L. S., Tapponnier, P., Duration of strike-slip movements in the large shear zones: The Red River belt, China, Earth Planet Sci. Lett., 1994, 126: 379—397.
16. Zhang, L. S., Schärer, U., Age and origin of magmatism along the Cenozoic Red River shear belt, Contrib. Mineral. Petrol., 1999, 134: 67—85.
17. Turner, S., Arnaud, N., Liu, J. Q. et al., Post-collision, shoshonitic volcanism on the Tibetan Plateau: Implications for convective thinning of the lithosphere and the source of ocean island basalts, J. Petrol., 1996, 37: 45—71.
18. Miller, C., Schuster, R., Klözli, U. et al., Post-collisional potassic and ultrapotassic activities in SW Tibet: Geochemical and Sr-Nd-Pb-O isotopic constraints for mantle source characteristics and petrogenesis, J. Petrol., 1999, 40: 1399—1424.
19. Wang, E., Burchfiel, B. C., Interpretation of Cenozoic tectonics in the right-lateral accommodation zone between the Ailao Shan shear zone and the eastern Himalayan syntaxis, Int. Geol. Rev., 1997, 39: 191—219.
20. Ratschbacher, L., Frisch, W., Chen, C. et al., Cenozoic deformation, rotation, and stress patterns in eastern Tibet and western Sichuan, China, in The Tectonic Evolution of Asia (eds. Yin, A., Harrison, T. M.), New York: Cambridge University Press, 1996, 227—249.
21. Xie, G. H., Liu, C. Q., Masuda, A. et al., The geochemical characteristics of Cenozoic volcanic rocks in the area of Qinghai-Tibet plateau: Evidence for existing of an ancient enriched mantle, in The Age and Geochemistry of Cenozoic Volcanic Rocks in China (ed. Liu, R. X) (in Chinese), Beijing: Seismological Press, 1992, 400—427.
22. Briais, A., Patriat, P., Tapponnier, P., Updated interpretation of magnetic anomalies and seafloor spreading stages in the South China Sea: Implications for the Tertiary tectonics of SE Asia, J. Geophys. Res., 1993, 98: 6299—6328.
23. Meyer, B., Tapponnier, P., Bourjot L. et al., Crustal thickening in Gansu-Qinghai, Lithospheric mantle subduction, and oblique, strike-slip controlled growth of the Tibet Plateau, Geophys. J. Int., 1998, 135: 1—47.
24. Wang, E., Burchfiel, B. C., Chen, L. Z. et al., Late Cenozoic Xianshuihe-Xiaojiang, Red River, and Dali Fault Systems of Southwestern Sichuan and Central Yunnan, China, Boulder (Colorado): GSA Inc., 1998, 1—108.
25. Lenardic, A., Kaula, W. M., More thoughts on convergent crustal plateau formation and mantle dynamics with regard to Tibet, J. Geophys. Res., 1995, 100: 15193—15203.
26. Rangin, C., Huchon, P., Le Pichon, X. et al., Cenozoic deformation of central and south Vietnam, Tectonophysics, 1995, 251: 179—196.
27. Armijo, R., Tapponnier, P., Han, T., Late Cenozoic right-lateral strike-slip faulting across southern Tibet, J. Geophys. Res.,

1989, 94: 2787—2838.

28. Harrison, T. M., Copeland, P., Kidd, W. S. F. et al., Activation of the Nyainqentanghla shear zone: Implications for uplift of the southern Tibetan Plateau, Tectonics, 1995, 14: 658—676.
29. Masek, J. G., Isacks, B. L., Fielding, E. J. et al., Rift flank uplift in Tibet: Evidence for a viscous lower crust, Tectonics, 1994, 13: 659—667.
30. Chen, W. P., Kao, H., Seismotectonics of Asia: Some recent progress, in The Tectonic Evolution of Asia (eds. Yin, A., Harrison, T. M.), New York: Cambridge University Press, 1996, 37—52.
31. Yin, A., Mode of Cenozoic east-west extension in Tibet suggesting a common origin of rifts in Asia during the Indo-Asian collision, J. Geophys. Res., 2000, 105: 21745—21759.
32. Delvaux, D., Moeys, R., Stapel, G. et al., Paleostress reconstructions and geodynamics of the Baikal region, Central Asia, Part 2: Cenozoic rifting, Tectonophysics, 1997, 282: 1—38.
33. Flower, M., Tamaki, K., Hoang, H., Mantle extrusion: A model for dispersed volcanism and DUPAL-like asthenosphere in east Asia and the western Pacific, in Mantle Dynamics and Plate Interactions in East Asia (eds. Flower, M. F. J., Chung, S. L., Lo, C. H.), Washington D.C.: AGU, 1998, Geodynamics Ser. 27: 67—88.
34. Hoang, N., Flower, M. F. J., Petrogenesis of Cenozoic basalts from Vietnam: Implications for origin of a “diffuse igneous province”, J. Petrol., 1998, 39: 369—395.